Available online at www.sciencedirect.com
SCIENCE DIRECT®
Spectrochimica Acta Part A 59 (2003) 3325–3335
SPECTROCHIMICA ACTA PART A
www.elsevier.com/locate/saa

Experimental and computational studies of the structure and vibrational spectra of 2-[5,5-dimethyl-3-(2-phenyl-vinil)-cyclohex-2-enylidene]-malononitrile

Tsonko M. Kolev *, Denitsa Y. Yancheva, Bistra A. Stamboliyska

Institute of Organic Chemistry, Bulgarian Academy of Sciences, Bonchev str., Buld. 9, Sofia 1113, Bulgaria

Received 5 February 2003; received in revised form 19 March 2003; accepted 20 March 2003

Abstract

The FTIR spectra (4000–100 cm^{-1}) and Raman spectra (3500–30 cm^{-1}) of 2-[5,5-dimethyl-3-(2-phenyl-vinil)-cyclohex-2-enylidene]-malononitrile in solid state were measured. In addition, the structure and harmonic vibrational frequencies of this molecule were theoretically evaluated using B3LYP density functional methods. The computed vibrational frequencies are used to determine the types of molecular motions associated with each of the experimental bands observed. Bond length alternation (BLA) was established. Comparison with the experimental spectra provides important information about the ability of this computational method to describe the vibrational modes in this type of ''push–pull'' systems with potential non-linear optical applications.

Keywords: Vibrational spectra; Density functional theory; Force field; Electronic structure; Band assignment; Non-linear optics

1. Introduction

Accurate vibrational assignment for aromatic and another conjugated systems is necessary for characterization of materials. Assignments for complex systems can be proposed on the basis of frequency agreement between the computed harmonics and the observed fundamentals. Density functional theory (DFT) is becoming increasingly popular among experimentalists and theoreticians in the present chemical literature [1,2]. Numerous reports have been made citing the success of DFT compared with the conventional ab initio methods in computing molecular and chemical properties such as geometries, harmonic frequencies, and energies [3–6]. DFT is superior to the conventional methods such as Hartree–Fock (HF) and second-order Møller–Plesset perturbation theory (MP2), for the calculation of polyatomic vibrational frequencies with empirical scaling factors approaching unity [4,5]. The cost effectiveness of DFT over conventional methods is an additional feature. This method we were employed in our spectroscopic and theoretical investigations of the new organic material for non-linear optical, elec-

* Corresponding author. Tel.: +359-2-960-6106; fax: +359-2-700-225.
E-mail address: kolev@orgchm.bas.bg (T.M. Kolev).

1386-1425/03/$ - see front matter © 2003 Elsevier B.V. All rights reserved.
doi:10.1016/S1386-1425(03)00140-9

tro-optical and photorefractive applications namely 2-[5,5-dimethyl-3-(2-phenyl-vinyl)-cyclohex-2-enylidene]malononitrile (DPCM) (Scheme 1). The compound has been synthesized and described by Lemke [7]. In the recent years Wortmann et al. have shown the utilization of the chromophore DPCM in a novel sensitized photochromic organic glass for holographic optical storage. The recording mechanism involves a triplet-sensitized photoreaction of this organic chromophore [8]. DPCM exhibits a high first-order anisotropic polarizability along the polyenic backbone, arising from the intense absorption band at $\lambda_{max} = 394$ nm (chloroform) with oscillator strength of $f = 0.92$. The authors have found that the intense absorption band is not present in the spectrum of photoproduct, resulting in a substantial change in the optical polarizability during the photoreaction [8]. All these interesting features of DPCM are a motivation for a detailed investigation of its electronic structure and vibrational spectra by means of DFT method. On the other hand the compounds from this type as *p*-OH substituted DPCM form resonance-stabilized anion exhibiting a strong negative solvatochromism [7]. The basic method for exploring compounds with such properties is electric field induced second harmonic generation (EFISH) [9,10]. The compound with *p*-$N(CH_3)_2$ group shows $\lambda_{max} = 519$ nm (*N*-methylpyrrolidine-1-on); the value of the molecular hyperpolarizability is $\beta = 246 \times 10^{-30}$ esu, dipole moment (μ) 8.7 Debye using laser with wavelength of 1907 nm [11]. The resulting value of β (1907 nm) was extrapolated to zero frequency (β_0) using the two-level-model of Oudar and Chemla [12].

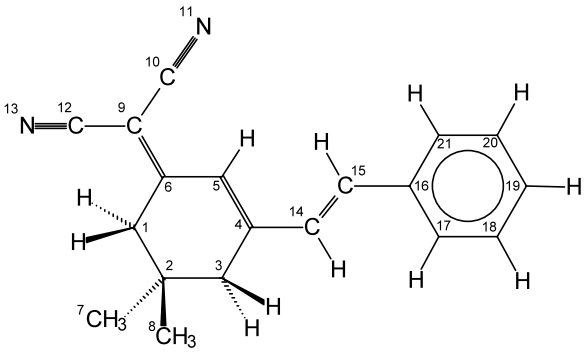

Scheme 1. Molecule diagram of 2-[5,5-dimethyl-3-(2-phenyl-vinyl)-cyclohex-2-enylidene]-malononitrile including atomic numbering scheme.

DPCM molecule is the simplest representative of this type of compounds. The UV–vis spectral data show that these materials have also a potential non-linear optical (NLO) activity. As it is known the hyperpolarizability of an organic molecule is related to the charge transfer (CF) characteristics eventually governed by the increasing conjugation length and strength of the donor and acceptor groups. Both the second-order optical non-linearity and the optical transparency are affected by the nature of the conjugated bonds, the length of π-conjugation, the strength of electron donor and acceptor substituents, and the conformations. In the concerning case the lengths of the three double bonds are equalized in great extend, which is a good prerequisite for large β-values. The measured β-values for similar trienic systems are of the magnitude of $\beta = 135 \times 10^{-30}$ esu [9]. The studied molecule has $\lambda_{max} = 389.5$ nm (EtOH) and 394 nm ($CHCl_3$), $\lambda_{cut\ off} = 480$ nm (EtOH). Accordingly the terms of non-linearity–transparency trade-off [10] this trienic conjugated chain is advantageous because there is a combination of a weak donor (phenyl) and a very strong acceptor (dicyanomethylene) end groups and the relevant compound could be possibly used for non-linear optical applications.

We found any vibrational investigation in the literature for the certain molecule.

In this work we report the results from FTIR and Raman spectra in solid state and the results from the DFT calculations on the structure and the harmonic force field of titled compound. Assignments of fundamental molecular vibrations are performed on the basis of the DFT (B3LYP/6-31G*) quantum chemical calculations.

2. Experimental

The title compound was synthesized using a general procedure described by Lemke [7]. The preparation of the starting compound 3,5,5-trimethyl(cyclohex-2-enylidene)malononitrile is de-

scribed in one of our previous paper [13]. The IR spectra of the studied compound were recorded in the solid state in CsI, KBr pellets and in CCl_4 solutions on a Bruker IFS-113v spectrometer equipped with high intensity Globar source Ge/KBr beam splitter, and TGS detector. The far IR spectra were recorded on the same model spectrometer equipped with high-pressure Hg arc lamp a 6.25 or 25 μm Mylar beam splitter and DTGS detector. In both cases the spectra were recorded at a resolution of 1 cm^{-1} (100 scans). The Raman spectra were recorded as a powder in capillary tube at room temperature on Jobin–Ivone 64000 spectrometer using 647.10 nm laser excitation with 100 mW power in the 4000–30 cm^{-1} frequency region.

3. Computations

DFT is used to obtain equilibrium geometry, force field and fundamental vibrational frequency of DPCM-molecule. All calculations have been performed with the standard GAUSSIAN [14] software (AIX, version 1998). DFT method, employed in the present study is B3LYP-Becke's three-parameter hybrid method [15] using the correlation functional of Lee, Yang and Parr [16]. The standard 6-31G* basis set was applied in the calculations. We have studied only the conformer, which corresponds to the X-ray data for the *p*-Me derivative of DPCM. The stationary points found on the molecular potential energy hypersurfaces were characterized using standard analytical harmonic vibrational analyses. The absence of negative frequencies, as well as negative eigenvalues of the second-derivative matrix confirmed that the stationary points correspond to minima on the potential energy hypersurfaces. It is well known that B3LYP method overestimates the frequencies of fundamental vibrations significantly. Thus, for a better correspondence between experimental and calculated values, the B3LYP results were modified using the empirical scaling factor—0.9614, reported by A.P. Scott and L. Radom [4].

4. Results and discussion

4.1. Vibrational assignment

In this study we take into account the respective activity of all bands in IR and Raman spectra due to the presence of C_1 symmetry of the isolated DPCM molecule.

The fragment of IR spectrum of DPCM in 3200–2700 cm^{-1} region, in CsI pellet is shown in Fig. 1. The middle IR spectrum of the same compound in KBr disc is presented in Fig. 2. The FIR spectrum in CsI matrix in 500–100 cm^{-1} region is shown in Fig. 3. The Raman spectrum of DPCM in solid phase as microcrystalline powder in glass capillary is given in Fig. 4. The numeric values of experimental frequencies are compared with the corresponding B3LYP/6-31G* data in Table 1. The computed vibrational frequencies are used to determine the types of molecular motion associated with each of the observed experimental bands. The assignment of the vibrational modes of the phenyl moiety is denoted by means of Wilson's nomenclature [17], whereas the forms of the vibrations of remaining part of molecule are described approximately. In the description of complex vibrations the vibrational motions of the greatest amplitude are given. The agreement of the calculated frequencies with the experimental data (Table 1) is very good. The absolute mean deviation between experimental and theoretical IR data is 8.5 cm^{-1}.

4.1.1. Vibrational assignment of phenyl moiety

Assignment of the phenyl bands in the experimental spectrum is carried out on the base of previous work for mono-substituted benzenes [17–19], as well as calculations presented here. Five stretchings ν_{CH} viz. **20a**, **20b**, **2**, **7b** and **13** were observed in the IR spectrum of the DPCM. The band corresponding to **13** vibration is predicted by B3LYP/6-31G* method as band with zero intensity, but in the experimental spectrum it was found at 3060 cm^{-1} as a very weak band. The frequencies of ν_{CH} vibrations indicate a general trend toward slight increase compared with the literature data for standard mono-substituted benzenes without CT. Unlike the slightly increased frequen-

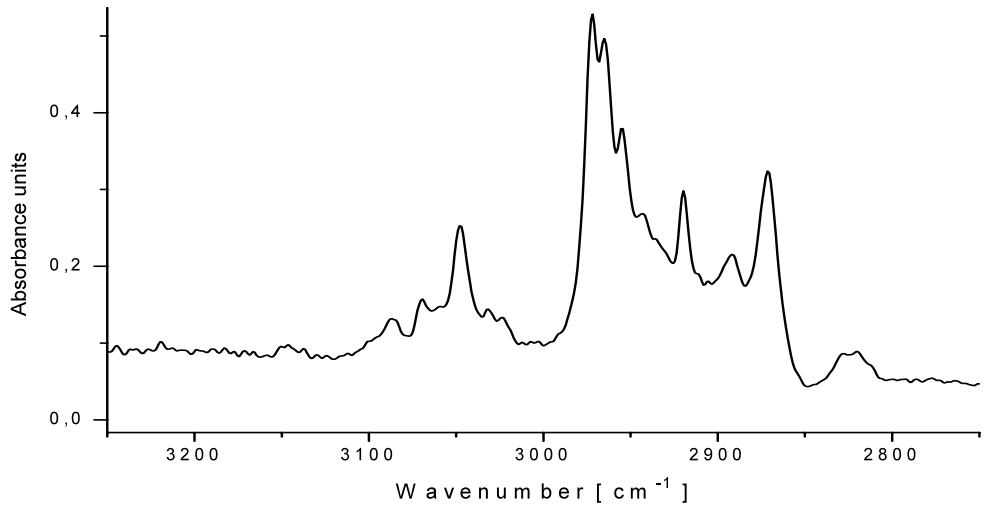

Fig. 1. IR spectrum of DPCM (6 mg in 250 mg CsI) pellet in 3250–2750 cm^{-1} frequency region.

cies, the intensities of the corresponding bands are significantly decreased probably due to the presence of CT in the molecule.

The normal vibrations of predominantly CC character viz. **8a**, **8b**, **19a**, **19b** and **14** are predicted correctly by B3LYP/6-31G*, mean deviation 8 cm^{-1}. The band belonging to **8b** vibration is strongly overlapped with the most intensive band at 1566 cm^{-1} in the Raman and at 1567 cm^{-1} in the IR and, therefore, the frequency of **8b** cannot be determined precisely. The coincidence between experimental and predicted frequencies for **19a** and **19b** vibrations is very good (see Table 1).

Generally the theory fails with the description of the form and the frequency of vibration **14** (“Kekule”) [20–22]. In this case the frequency as well as the form of the mode **14** are predicted correctly—the calculated frequency is 1320 cm^{-1} and the found: 1332 cm^{-1} in the IR and 1331 cm^{-1} in the Raman.

The C–H-in-plane deformation vibrations: **3**, **9a**, **9b**, **15**, **18a** in the experimental spectrum are

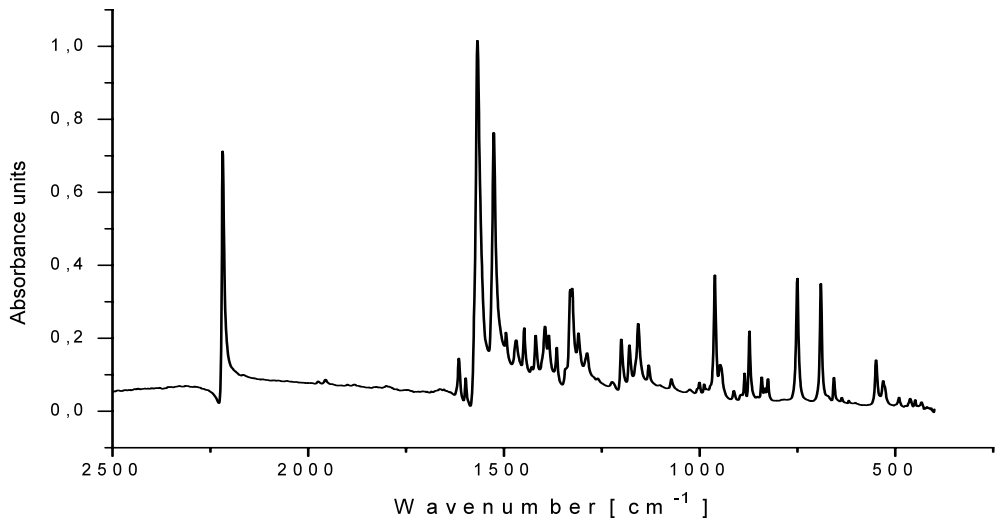

Fig. 2. Middle IR spectrum of DPCM in KBr pellet in 2500–400 cm^{-1} frequency region.

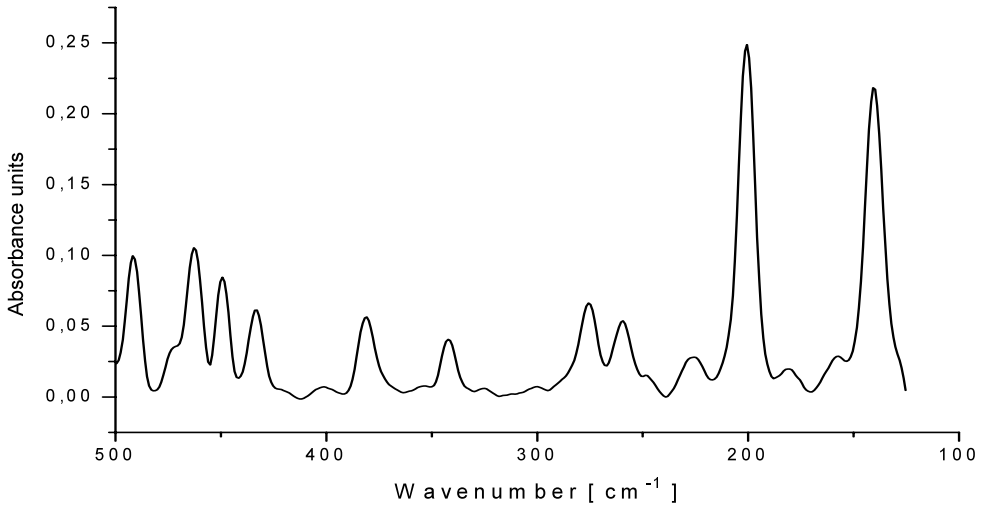

Fig. 3. Far IR spectrum of DPCM (6 mg) in CsI (250 mg) in 500–100 cm^{-1} frequency region.

found in the frequency region of 1325–1072 cm^{-1}, which is in agreement with theoretical data (Table 1), e.g. the calculated frequency of the normal mode **18a** is at 1074 cm^{-1} and it is measured at 1072 cm^{-1} (IR).

The frequency of normal mode **1** (“breathing”) is well predicted by theory—calculated 1017 cm^{-1}, found 1025 cm^{-1}. The predicted form of this normal mode has predominantly δ_{CCC} character.

The frequency region of C–H-out-of-plane deformation vibrations **5**, **17a**, **17b**, **10a**, **11** is predicted correctly also 989–736 cm^{-1}, measured 988–740 cm^{-1}. It can be emphasized that the

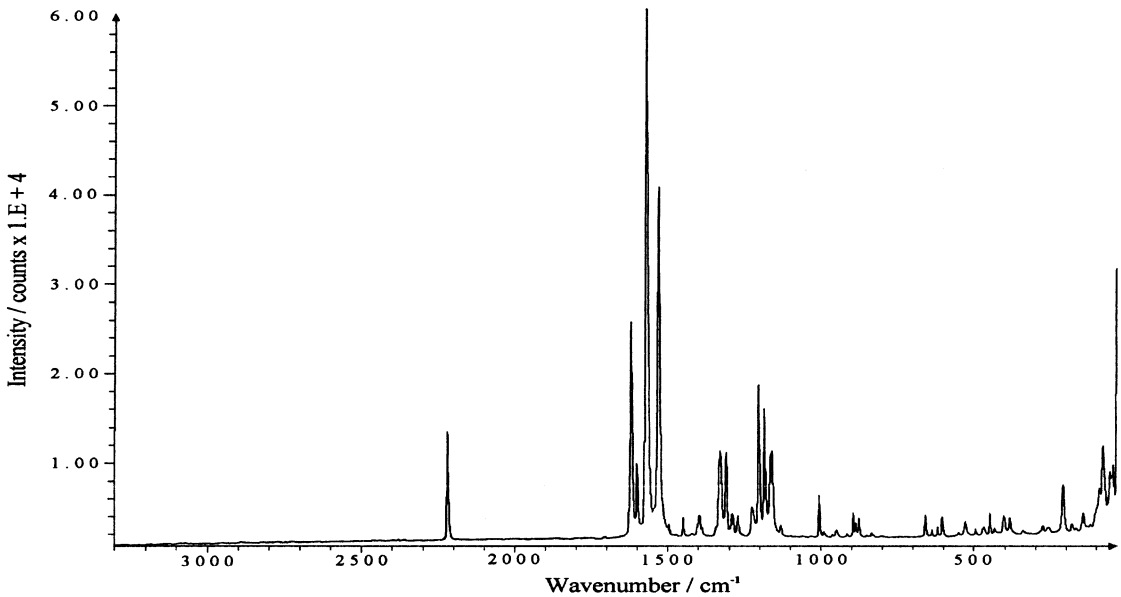

Fig. 4. Raman spectrum of DPCM in capillary tube in 4000–30 cm^{-1} frequency region at room temperature, 647.10 nm laser excitation, 100 mW power.

Table 1
Comparison of calculated and observed spectra for DPCM

B3LYP frequency (cm^{-1})	B3LYP[a]scaled (cm^{-1})	IR intensity (km mol^{-1})	IR frequency (cm^{-1})	Raman frequency (cm^{-1})	Approximate description[b]
3216	3092	33.7	3091		**20a**
3208	3084	31.2	3087		**20b**
3207	3083	2.6			$\nu(C^5–H)$
3199	3076	5.7			**2**
3190	3067	0.0	3069		**13**
3185	3062	6.5	3060		**7b**
3172	3050	29.4	3048		ν^{as}(H–CC–H)
3164	3042	3.2	3032		ν^{s}(H–CC–H)
3128	3007	29.5	3023		$\nu^{as}(CH_3)$
3116	2996	36.3	3003		$\nu^{as}(CH_3)$
3110	2990	14.0			$\nu^{as}(CH_3)$
3107	2987	21.8	2972		$\nu^{as}(CH_3)$
3101	2981	3.3	2965		$\nu^{as}(C^1H_2)$
3057	2939	24.7	2943		$\nu^{as}(C^3H_2)$
3050	2932	13.3	2934		$\nu^{s}(C^1H_2)$
3041	2924	29.5	2920		$\nu^{s}(CH_3)$
3016	2900	11.7	2892		$\nu^{s}(C^1H_2)$
3007	2891	14.8	2871		$\nu^{s}(C^3H_2)$
2337	2247	107.9			ν^{as}(CN)
2322	2232	28.2	2218	2218	ν^{s}(CN)
1687	1622	43.4	1615	1617	$\nu(C^{14}=C^{15})$
1659	1595	5.6	1598	1599	**8a**
1633	1570	19.0	Overl.	overl.	**8b**
1607	1545	468.8	1567	1566	$\nu(C^4=C^5)$
1566	1506	283.9	1525	1527	$\nu(C^6=C^9)$
1545	1485	3.1	1494	1496	**19a**
1541	1482	3.2	1468		$\delta(CH_3)$
1535	1476	3.3			$\delta(CH_3)$
1523	1464	5.0			$\delta(CH_3)$
1517	1458	1.2			$\delta(CH_3)$
1499	1441	5.4			$\delta(C^1H_2)+\delta(C^3H_2)$
1498	1440	29.3	1448	1449	**19b**
1489	1432	9.4	1418	1419	$\delta(C^1H_2)+\delta(C^3H_2)$
1452	1396	5.2	1395	1396	$\delta(CH_3)$
1431	1376	6.5	1385	1388	$\delta(CH_3)$
1424	1369	43.7	1365		$\delta(C^4C^5H)+\delta(C^3H_2)$
1394	1340	2.4			$\delta(C^1H_2)+\delta(C^3H_2)$
1380	1327	3.7			$\delta(HC^{14}C^{15})$
1373	1320	11.8	1332	1331	**14**
1366	1313	186.5	1325	1327	$\delta(C^4C^5H)+\delta(HC^{14}C^{15})$
1356	1304	2.8	1309	1309	**3**
1336	1284	8.1	1287	1288	$\delta(C^1H_2)+\delta(C^3H_2)$
1333	1282	8.8			$\nu(C^{15}–C^{Ph})$-**12**(X)
1318	1267	9.7	1260	1270	$\delta(HC^{14}C^{15})+\delta(C^4C^5H)$
1298	1248	0.3			$\nu(C^2–C^{Me})+\delta(C^3H_2)$
1262	1213	2.2	1224	1224	**9a**$+\delta(HC^{14}C^{15})$
1230	1183	2.7	1199	1202	$\delta(C^1C^2C^3)+\delta(CH_3)$
1218	1171	1.45	1179	1183	**9b**
1205	1158	8.8		1165	$\delta(C^6C^9C)$
1200	1154	14.9	1156	1159	$\gamma(C^1H_2)+\gamma(C^3H_2)$
1195	1149	0.5			**15**

Table 1 (*Continued*)

B3LYP frequency (cm^{-1})	B3LYP[a]scaled (cm^{-1})	IR intensity (km mol^{-1})	IR frequency (cm^{-1})	Raman frequency (cm^{-1})	Approximate description[b]
1169	1124	63.9	1130	1131	
1165	1120	9.2			$\gamma(C^1H_2)+\gamma(CH_3)$
1117	1074	2.9	1072		**18a**
1058	1017	1.1	1025		**1**
1049	1009	0.1	1000	1003	$\gamma(CH_3)$
1029	989	1.5	988	989	**5**
1017	978	20.3			$\gamma(HC^{14}C^{15})$
1015	976	12.8			**17a**
1010	971	3.6	961	960	$\gamma(C^1C^5H)$, $\gamma(HC^{14}C^{15})$
997	959	5.4	947	949	**17b**
968	931	0.1			
960	923	0.8			$\gamma(CH_3)$
944	908	6.8		914	$\nu(C^2-C^3)+\delta(C^1C^2C^3)$
937	901	1.5		893	$\gamma(C^1H_2)+\gamma(CH_3)$
934	898	3.4			$\gamma(C^1C^5H)+\gamma(C^{Ph}H)$
928	892	11.8	885	886	$\gamma(C^1C^5H)+\gamma(C^{Ph}H)$
917	882	0.4	872	876	$\gamma(C^3H_2)+\gamma(CH_3)$
907	872	6.4		852	$\gamma(C^{Ph}H)+\gamma(C^3H_2)$
873	839	1.3	841	845	$\gamma(C^{Ph}H)+\gamma(HC^{14}C^{15})$
866	833	4.1	833	835	$\gamma(C^{Ph}H)+\delta(C^2C^3C^4)$
849	816	0.1	825	828	**10a**
844	811	0.6			$\delta(C^6C^5C^4)$
777	747	7.8	750		$\gamma(C^{Ph}H)+\gamma(C^1H_2)+\gamma(CH_3)$
766	736	25.2			**11**
701	674	22.9	690		**4**
685	659	3.2	656	658	$\delta(C^{12}C^9C^{10})$
665	639	2.1	636	638	$\delta(C^{12}C^9C^{10})$
633	609	0.3	618	619	**6a**
613	589	0.2	603	603	δ(NCC)
565	543	5.7	549	550	$\gamma(C^1C^5H)+\gamma(C^1H_2)$
564	542	4.1	531	528	$\delta(C^9C^6C^1)+\delta$(NCC)
540	519	1.8			$\gamma(C^1H_2)+\gamma(C^1C^5H)$
534	513	3.2	490	495	**6b**
505	486	3.1			$\gamma(C^{Ph}H)+\delta$(skel.)
482	463	0.2	462	466	τ(NCCC)
469	451	3.8	449	448	**16a**
465	447	1.3	433	433	γ(NCC)$+\gamma(C^1H_2)$
431	414	0.8	403	403	$\delta(C^1C^2C^3)+\delta(C^7C^2C^8)$
412	396	0.0			**16b**
405	389	0.5	381	382	$\delta(C^8C^2C^3)+\delta(C^7C^2C^8)$
391	376	2.2			$\tau(HC^{14}C^{15}H)+\tau$(NCCC)
342	329	2.3	342	342	$\delta(C^2C^3C^4)+\delta(C^3C^4C^5)$
325	312	0.2	275	277	$\delta(C^1C^2C^4)+\gamma(C^1H_2)$
281	270	1.0	259	261	$\tau(HC^8C^2C^1)$
279	268	1.2		256	$\tau(HC^7C^2C^1)$
251	241	2.8			$\tau(HC^8C^2C^3)$
234	225	4.3	227		$\tau(HC^{14}C^{15}H)$
226	217	0.6			$\tau(HC^8C^2C^1)+\tau(HC^7C^2C^1)$

Table 1 (*Continued*)

B3LYP frequency (cm^{-1})	B3LYP[a]scaled (cm^{-1})	IR intensity (km mol^{-1})	IR frequency (cm^{-1})	Raman frequency (cm^{-1})	Approximate description[b]
218	210	1.6		209	$\tau(HC^8C^2C^1)+\tau(HC^7C^2C^1)$
189	182	2.4	181	180	$\tau(HC^5C^6C^1)$
172	165	1.6	158		**10b**(X)
152	146	2.2	140	143	$\tau(HC^{14}C^{15}H)$
128	123	6.6			$\delta(C^{10}C^9C^{12})$
114	110	1.9			$\gamma(C^{10}C^9C^{12})$
89	86	0.7		88	$\tau(HC^{14}C^{15}H)+\gamma(C^{Ph}H)$
69	66	0.6		78	γ(skelet.)
57	55	0.9		53	τ(skelet.)
43	41	1.3		43	$\tau(nccc^6)$
32	31	0.1		30	τ(Ph)
16	15	0.2			τ(Ph)

[a] Scaled by 0.9614 [4].
[b] Vibrational modes: ν, stretching; δ and γ, in-plane and out-of-plane bending, respectively; τ, torsion. Wilson's notation is used for the phenyl modes.

band at 750 cm^{-1} overlaps the expected one of vibration **11** ("umbrella" mode) in IR spectrum.

Three or even more of the ring vibrations of phenyl are substituent-sensitive and their utility for identification purposes is limited. They are strongly coupled to the phenyl-X (substituent) stretching vibration and an interchange with the latter is not excluded [18,19]. A good agreement between the computed and experimental frequencies of these modes is found in accordance with the literature data [18,19,21,22]. Calculated ring vibrations lay in the 674–165 cm^{-1} region, measured: 690–158 cm^{-1}.

4.1.2. Vibrational assignment of cycloaliphatic moiety

The stretching C–H vibrations of aliphatic part are at higher frequencies as usual [18]. The extremely high value of $\nu(C^5–H)$, calculated at 3083 cm^{-1} is weakly intensive. It is probably overlapped with the band at 3087 cm^{-1} (IR).

The ethylenic ν^{as} and ν^{s} (H–CC–H) are predicted well-found at 3048 and 3032 cm^{-1}. The experimentally found frequencies lay in the region where usually appear aromatic ν(C–H) vibrations. The presence of CT in the molecule of DPCM causes the increase of ν(C–H) of the two linkers (ethylenic C–H) and a slow decrease of their intensities. The $\nu(CH_2)$ and $\nu(CH_3)$ frequencies of the groups, which are out of conjugation, are not affected significantly.

Stretching vibrations corresponding to the three double CC bonds viz. $\nu(C^{14}=C^{15})$, $\nu(C^4=C^5)$ and $\nu(C^6=C^9)$ lay in 1622–1506 cm^{-1} frequency range (B3LYP/6-31G*). We found these vibrations in 1615–1525 cm^{-1} (IR). In the Raman spectrum the frequency region is practically the same (1617–1527 cm^{-1}). The calculated intensities of these bands correspond in great extend to the measured ones e.g. the most intense band in the theoretical spectrum at 1545 cm^{-1} ($A = 468$ km mol^{-1}) corresponds to the most intense bands at 1567 cm^{-1} (IR) and 1567 cm^{-1} (Raman). The frequency and the intensity of the second intense band in IR and Raman spectra have also very good coincidence with the theoretical one (1506 cm^{-1}, $A = 283$ km mol^{-1}) assigned to $\nu(C^6=C^9)$.

The used theoretical method forecasts two bands, belonging to symmetric and asymmetric vibrations of the cyano groups with 15 cm^{-1} split between ν^{s}(CN) and ν^{as}(CN). In both IR and Raman spectra only one band at 2218 cm^{-1} appears. The reasonable cause for the lack of splitting of this band in the experimental spectra cannot be found so far.

4.2. Structure

The bond lengths and bond angles calculated by means of B3LYP method are presented together with the corresponding data from X-ray analysis of *p*-Me analogue in Table 2. The general trend to increase the single C–C bond lengths and to decrease the double C=C bond lengths of the conjugated main backbone is observed. As can be seen in Table 2 the bond length of C^6=C^9, C^5=C^4 and ethylenic bridge C^{14}=C^{15} are near to the aromatic one, while single bonds C^9–C^{10}, C^6–C^5, C^4–C^{14}, C^{15}–C^{16} are shorter than the single C–C one. The bond length alternation (BLA) in linear chains of D···A substituted compounds is an important indicator for the performance of NLO-phores [23]. It is defined as a mean difference between the lengths of formal C–C and C=C bonds. Its degree is a consequence of the extent of coupling between donor and acceptor end group. Similarly degree of BLA was experimentally observed in the X-ray structure of *p*-methyl derivative [24]. The calculated value of the dipole moment of the studied compound is 8.80 Debye, larger than the paradigmatic molecule of *p*-nitro aniline [25,26]. The main reason for this increment is the charge flux (intramolecular CT), which creates a large permanent dipole moment.

The net electronic charges of the non-hydrogen atoms belonging to the conjugated π-system are as follow: N^{11}: −0.492; C^{10}: 0.291; C^9: 0.032; C^6: 0.213; C^5: −0.239; C^4: 0.173; C^{14}: −0.193; C^{15}: −0.162; C^{16}: 0.171; C^{17}: −0.173; C^{18}: −0.131; C^{19}: −0.124; C^{20}: −0.129; C^{21}: −0.190.

In accordance with the electron drawing character of dicyanomethylene group a large part of the electron density is localized over it. The atomic charge over C^4 atom is 0.1728, while this one over C^5 is −0.2397. We consider that this charge alternation in the C^4=C^5 bond is the reason for the extremely high intensity of the band corresponding to the $\nu(C^4{=}C^5)$ vibration. In difference to charge distribution in the discussed bond, atomic charges over C^{14} and C^{15} have equal signs of atomic charges and similar values which causes very probably the lower intensity of this band in comparison with $\nu(C^4{=}C^5)$ mode.

Table 2
Theoretical (B3LYP/6-31G*) bond lengths (Å) and bond angels (°) of DPCM compared with X-ray data of *p*-Me-DPCM[a]

	B3LYP	Experimental [24]
Bonds		
C^1–C^2	1.546	1.526
C^2–C^3	1.545	1.527
C^2–C^7	1.542	1.532
C^2–C^8	1.538	1.530
C^3–C^4	1.515	1.487
C^4–C^5	1.368	1.343
C^5–C^6	1.433	1.421
C^6–C^1	1.510	1.494
C^6–C^9	1.383	1.362
C^9–C^{10}	1.430	1.424
C^{10}–N^{11}	1.165	1.144
C^9–C^{12}	1.429	1.432
C^{12}–N^{13}	1.165	1.136
C^4–C^{14}	1.455	1.462
C^{14}–C^{15}	1.356	1.311
C^{15}–C^{16}	1.460	1.473
C^{16}–C^{17}	1.410	1.400
C^{17}–C^{18}	1.390	1.383
C^{18}–C^{19}	1.399	1.376
C^{19}–C^{20}	1.396	1.372
C^{20}–C^{21}	1.393	1.366
C^{21}–C^{16}	1.409	1.376
Angles		
$<(C^1C^2C^3)$	108.0	108.3
$<(C^1C^2C^7)$	110.4	108.9
$<(C^1C^2C^8)$	109.2	109.9
$<(C^2C^3C^4)$	114.6	114.2
$<(C^3C^4C^5)$	120.3	120.4
$<(C^3C^4C^{14})$	116.5	117.9
$<(C^4C^5C^6)$	122.8	123.5
$<(C^4C^{14}C^{15})$	126.0	126.7
$<(C^5C^4C^{14})$	123.2	121.7
$<(C^5C^6C^1)$	118.1	117.6
$<(C^5C^6C^9)$	121.2	121.0
$<(C^6C^1C^2)$	113.1	112.9
$<(C^6C^9C^{10})$	121.7	120.3
$<(C^6C^9C^{12})$	121.8	122.6
$<(C^9C^{10}C^{11})$	180.0	178.9
$<(C^9C^{12}C^{13})$	180.0	179.4
$<(C^{12}C^9C^{10})$	116.4	117.0
$<(C^{14}C^{15}C^{16})$	127.3	126.8
$<(C^{15}C^{16}C^{17})$	123.5	122.4
$<(C^{16}C^{17}C^{18})$	120.8	120.2
$<(C^{17}C^{18}C^{19})$	120.4	121.4
$<(C^{18}C^{19}C^{20})$	119.7	117.6
$<(C^{19}C^{20}C^{21})$	119.9	121.7
$<(C^{21}C^{16}C^{17})$	118.0	117.4

[a] For atom numbering see Scheme 1.

It is known that the strength of the electron donating and accepting groups is expected to have an influence also on the geometric structure of the π-system as well as on the vibrational properties of the bridge. Relationship between intensities in IR, Raman and hyper-Raman spectra, and NLO properties of organic molecules have been studied [25–27]. On a more intuitive level the correspondence between vibrational frequencies and bond order could also be used. BLA in linear chains of D-linker-A compounds (one-dimensional NLO-phores) have been considered to be crucial indicator for the performance of NLO-phores [28,29]. It is defined as the mean difference between the length of formal C–C and double C=C bonds. Its order is a consequence of the extent of a coupling between a donor and acceptor end group. It may be of practical use if β values could be estimated from structural parameters directly [25,27,30]. It should be noted that some authors have questioned the predictable power of the concept for the development of new NLO-phores on the basis of quantum mechanical computations and theoretical considerations [31]. Nevertheless we consider that the estimation of BLA and β on the basis of the structural parameters of the conjugated molecules could serve as a reliable and fast theoretical method.

On the other hand from the expression of the static vibrational hyperpolarizability within the double harmonic approximation it appears that the largest contributions to vibrational hyperpolarizability come from those normal modes that have the largest intensities both in IR and Raman spectra [27,30]. Del Zoppo et al. [25] and Champagne [26] have studied NLO properties of the *p*-NA molecule and they found a few bands of vibrations contributing to vibrational hyperpolarizability, which are simultaneously strong in IR and Raman spectra. We consider the very strong bands at 1567, 1525 cm^{-1}, the strong ones at 1615 and 2218 cm^{-1} (IR), the very strong bands at 1566, 1527 cm^{-1}, strong ones at 1617 and 2218 cm^{-1} (Raman) corresponding to the vibrations already mentioned can be used for estimation of vibrational hyperpolarizability of DPCM and for its comparison with electronic one.

5. Conclusions

The bands in IR and Raman spectra of DPCM were assigned with the help of DFT force field calculations. The majority of the experimental frequencies is very well reproduced by the B3LYP/6-31G* method. Comparison of the theoretical and experimental spectra provides important information about the ability of above mentioned computational methods to describe the vibrational modes of this "push–pull" CF molecule with potential non-linear optical applications. BLA in polyenic backbone of the title compound was found and it can serve for estimation of first hyperpolarizability β. The molecular geometry of DPCM was compared with X-ray data for its *p*-Me analogue. The vibrational analysis of title compound gives results in agreement with those for similar compounds in literature. The most intensive normal modes in IR and Raman spectra having the largest contributions to vibrational hyperpolarizability have been found experimentally and also predicted theoretically.

Acknowledgements

This work has been supported financially by DAAD program "Stability Pact for South-Eastern Europe", Germany, Bulgarian National Fund of Scientific Research, Contract X-1213. One of us (T.M. Kolev) thanks the Alexander von Humboldt Stiftung-Bad Godesberg (Germany) for financial support.

References

[1] W. Kohn, A.D. Becke, R.G. Parr, J. Phys. Chem. 100 (1996) 12974.
[2] R.G. Parr, W. Yang, Density-Functional Theory of Atoms and Molecules, Oxford University Press, New York, 1989.
[3] B.G. Johnson, P.M.W. Gill, J.A. Pople, J. Chem. Phys. 98 (1993) 5612.
[4] A.P. Scott, L. Radom, J. Phys. Chem. 100 (1996) 16502.
[5] M.W. Wong, Chem. Phys. Lett. 256 (1996) 391.
[6] F. De Proft, G.M.L. Martin, P. Geerlings, Chem. Phys. Lett. 250 (1996) 393.
[7] R. Lemke, Chem. Ber. 103 (1970) 1894.

[8] R. Wortmann, P.M. Lundquist, R.J. Twieg, C. Geletneki, C.R. Moylan, Y. Jia, R.G. DeVoe, D.M. Burland, M.P. Bernal, H. Coufal, R.K. Grigier, J.A. Hoffnagle, C.M. Jefferson, R.M. Macfarlane, R.M. Shelby, G.T. Sincerbox, Appl. Phys. Lett. 69 (1996) 1657.
[9] H.S. Nalwa, S. Miyata (Eds.), Non-linear Optics of Organic Molecules and Polymers (Chapter 4), CRC Press, Boca Raton, 1997 (Chapter 4).
[10] D. Chemla, J. Zyss (Eds.), Non-linear Optical Properties of Organic Molecules and Crystals, vol. 1 and 2, Academic Press, New York, 1987.
[11] S. Ermer, S.M. Lovejoy, D.S. Leung, H. Warren, C.R. Moylan, R.J. Twieg, Chem. Mater. 9 (1997) 1437.
[12] J.L. Oudar, D.S. Chemla, J. Chem. Phys. 66 (1977) 2664.
[13] T. Kolev, Z. Glavcheva, D. Yancheva, M. Schuermann, D.C. Kleb, H. Preut, P. Bleckmann, Acta Crystallogr. Sect. E 57 (2001) o561.
[14] M.J. Frisch, G.W. Trucks, H.B. Schlegel, G.E. Scuseria, M.A. Robb, J.R. Cheeseman, V.G. Zakrzewski, J.A. Montgomery, Jr, R.E. Stratmann, J.C. Burant, S. Dapprich, J.M. Millam, A.D. Daniels, K.N. Kudin, M.C. Strain, O. Farkas, J. Tomasi, V. Barone, M. Cossi, R. Cammi, B. Mennucci, C. Pomelli, C. Adamo, S. Clifford, J. Ochterski, G.A. Petersson, P.Y. Ayala, Q. Cui, K. Morokuma, D.K. Malick, A.D. Rabuck, K. Raghavachari, J.B. Foresman, J. Cioslowski, J.V. Ortiz, A.G. Baboul, B.B. Stefanov, G. Liu, A. Liashenko, P. Piskorz, I. Komaromi, R. Gomperts, R.L. Martin, D.J. Fox, T. Keith, M.A. Al-Laham, C.Y. Peng, A. Nanayakkara, C. Gonzalez, M. Challacombe, P.M.W. Gill, B. Johnson, W. Chen, M.W. Wong, J.L. Andres, C. Gonzalez, M. Head-Gordon, E.S. Replogle, J.A. Pople, GAUSSIAN 98, Revision A.7, Gaussian Inc, Pittsburgh, PA, 1998.
[15] A.D. Becke, J. Chem. Phys. 98 (1993) 5648.
[16] C. Lee, W. Yang, R.G. Parr, Phys. Rev. B 37 (1988) 785.
[17] E.B. Wilson, Phys. Rev. 45 (1934) 427.
[18] G. Varsanyi, Assignment for Vibrational Spectra of Benzene Derivatives, Academic Press, New York, 1969.
[19] N. Roeges, A Guide to the Complete Interpretation of Infrared Spectra of Organic Structures, Wiley, Chichester, 1994.
[20] H. Lampert, W. Mikenda, A. Karpfen, J. Phys. Chem. A101 (1997) 2254.
[21] T. Kolev, B.A. Stamboliyska, Spectrochim. Acta A56 (1999) 119.
[22] T. Kolev, B.A. Stamboliyska, Spectrochim. Acta A58 (2002) 3127.
[23] J. Wolff, R. Wortmann, in: D. Bethell (Ed.), Advances in Physical Organic Chemistry: Organic Materials for Second-Order Non-linear Optics, vol. 32, Academic Press, New York, 1999.
[24] T. Kolev, D. Yancheva, M. Schürmann, D. Chr. Kleb, H. Preut, M. Spiteller, Acta Crystallogr. Sect. E 58 (2002) o1093.
[25] M. Del Zoppo, C. Castiglioni, G. Zerbi, Non-linear Opt. 9 (1995) 73; M. Del Zoppo, C. Castiglioni, P. Zuliani, G. Zerbi, Adv. Mater. 8 (1996) 345.
[26] B. Champagne, Chem. Phys. Lett. 261 (1996) 57.
[27] D. Bishop, Adv. Chem. Phys. 104 (1998) 1; D. Bishop, J. Pipin, B. Kirtman, J. Chem. Phys. 102 (1995) 6778.
[28] G. Bourhill, J.L. Bredas, L.T. Cheng, S.R. Marder, F. Meyers, J. Perry, B.G. Thiemann, J. Am. Chem. Soc. 116 (1994) 2619.
[29] C.B. Gormann, S.R. Marder, Chem. Mater. 7 (1995) 215.
[30] C. Castiglioni, M. Gussoni, M. Del Zoppo, G. Zerbi, Solid State Commun. 82 (1992) 13.
[31] R.J. Twieg, C.W. Dirk, Design, properties and applications of non-linear optical chromophores, in: F. Kajzar, J. Swalen (Eds.), Science and Technology of Organic Thin Films for Waveguiding Non-linear Optics, Gordon and Breach, Amsterdam, 1996, p. 45.